Acidity of dibasic carbon acids. Part 4.[1–3] Structure and ion solvation state of dimetallic salts of 9,10-dihydroanthracene and its derivatives in tetrahydrofuran

Malka Nir, Israel O. Shapiro, Roy E. Hoffman and Mordecai Rabinovitz *

Department of Organic Chemistry, The Hebrew University of Jerusalem, Givat Ram, Jerusalem, Israel 91904

The ion solvation state of dimetallic salts (M = Li–Cs) of 9,10-dihydroanthracene (DHA) and its derivatives in THF was studied by UV–VIS and NMR spectroscopies. The cations are situated on the opposite sides of the dianion plane in the dimetallic salts. Cation–dianion interaction stabilized the negative charge of the carbanion. The mechanism of dianion charge stabilization is affected by a phenyl substituent.

While organic synthesis widely uses the dimetallic salts of hydrocarbons,[4,5] information regarding their reactivity and the influence of cation, solvent and dianion structure on reactivity is very limited.[6,7] A measure of the dimetallic salts' reactivity is the second ionization constant (pK_2) of the corresponding dibasic hydrocarbon.[7] The first measurement of pK_2 of a dibasic hydrocarbon was achieved for 9,10-dihydroanthracene (DHA, 34.1 in cyclohexylamine with Cs^+ counter ion).[8] This value is close to that of diphenylmethane and its methyl derivatives.[9] The low reactivity of dimetallic salts of DHA was explained as being due to two reasons: extensive charge delocalization in the anion and strong anion–cation interaction.[7,8] Later we found that the pK_2 of DHA and its derivatives in tetrahydrofuran (THF) is very dependent on cation size.[1] These results show that information concerning the structures and ion solvation states of dimetallic salts of DHA and its derivatives is essential for understanding the influences of cation, solvent and dianion structure on their reactivity in solution.

The structure of $DHA^{2-}2Li^+$ has been studied using X-ray crystallography[10] and MNDO calculation.[11] According to both studies, the lithium ions are positioned on opposite sides of the anthracene plane, one over the central ring and the other under an outer ring (**I**).

The asymmetric structure of $DHA^{2-}2Li^+$ is related to the partial covalence of carbon–lithium bonding.[11] However, the structure of other dialkali metal salts of DHA is different when only coulombic interaction plays a role.[8,11] In this case the structure of dimetallic salts of DHA is symmetrical, with both cations being positioned over the central anthracene ring on opposite sides (**II**).

There is no information regarding the structure of dimetallic salts of DHA's derivatives.[12] Here we report the results of a study of the structure and ion solvation state of dimetallic salts of DHA and its derivatives in THF. The ion-solvation state study was carried out using UV–VIS and NMR spectroscopies. The structures were determined using the PM3 method.[13]

Results and discussion

Preparation of dimetallic salts of DHA and its derivatives

The dimetallic salts were prepared by exposure of anthracene and its 9,10-substituted derivatives to an alkali metal mirror under vacuum in THF. For dilithium salts, lithium wire was used. The reduction takes place in two stages: the formation of the anion radical, then the formation of the dianion [eqn. (1)],

$$A \xrightarrow{M,THF} A^{\bullet-}M^+ \xrightarrow{M,THF} A^{2-}2M^+ \qquad (1)$$

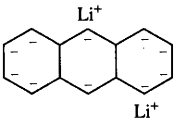

I

Structure of dilithium 9,10-dihydroanthracenediide

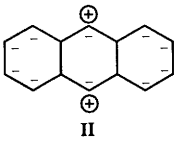

II

Structure of dimetallic salts of 9,10-dihydroanthracene other than lithium

where A is anthracene, 9-methylanthracene, 9-cyanoanthracene, 9-phenylanthracene, 9,10-dimethylanthracene or 9,10-diphenylanthracene; M is Li, Na, K, Rb or Cs.

Fig. 1 shows the structure and labelling of the dianions. All except a few of the salts are stable in THF over a wide temperature range. The dilithium salt of 9-phenyl-9,10-dihydroanthracene (PDHA) dimerizes over a few weeks in solution at room temperature to yield dilithium 9,9′,10,10′-tetrahydro-10,10′-diphenyl-9,9′-bianthracenyl-10,10′-diide. $DHA^{2-}2Li^+$ similarly polymerizes over a period of weeks while $DHA^{2-}2Na^+$ polymerizes over a period of years. $PDHA^{2-}$-$2Cs^+$ also reacts over a period of months although the reaction was not studied in detail.

Cation effect

The structure of solvated dimetallic salts of hydrocarbons is potentially more complex than that of monometallic salts. Several types of ion solvation are possible for dimetallic salts depending on cation size, solvent polarity and dianion structure. One possible structure is where the two cations are in direct contact with the dianion (contact ion triplet, CIT). Alternatively, a solvent shell surrounds the cation, separating the ions. In this case the solvent separated ion triplet (SSIT) is formed. A third possibility is where one cation is in contact and the other solvent separated (mixed ion triplet, MIT).[14,15] In addition to the above, free anions are possible, *i.e.* where the interionic distance is so large that the interionic interaction is negligible. Aggregation effects for dimetallic salts are more probable than for monometallic salts.[16]

For MIT, the two cations are in different states. We attempted to discover the existence of MIT using ^{23}Na NMR spectroscopy. However, the ^{23}Na NMR spectrum of

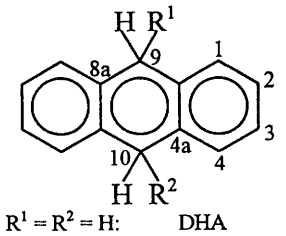

$R^1 = R^2 = H$: DHA
$R^1 = Me$; $R^2 = H$: MDHA
$R^1 = CN$; $R^2 = H$: CNDHA
$R^1 = Ph$; $R^2 = H$: PDHA
$R^1 = R^2 = Me$: DMDHA
$R^1 = R^2 = Ph$: DPDHA

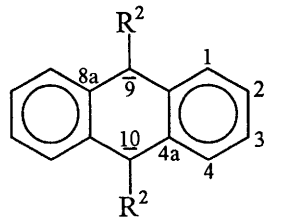

$R^1 = R^2 = H$: DHA^{2-}
$R^1 = Me$; $R^2 = H$: $MDHA^{2-}$
$R^1 = CN$; $R^2 = H$: $CNDHA^{2-}$
$R^1 = Ph$; $R^2 = H$: $PDHA^{2-}$
$R^1 = R^2 = Me$: $DMDHA^{2-}$
$R^1 = R^2 = Ph$: $DPDHA^{2-}$

Fig. 1 Structure and labelling of the dianions

$DPDHA^{2-}2Na^+$ only yields one peak that shifts from −8.5 ppm to −11.4 ppm as the temperature rises from 165 to 300 K. However, these results do not disprove the presence of MIT. It is known that the exchange between contact and solvent separated ion pairs of monometallic salts of organic compounds is much too fast for NMR spectroscopy to resolve, although UV–VIS spectroscopy may resolve it.[17] The single ^{23}Na lines therefore demonstrate a limitation of the NMR method rather than proving the absence of MIT.

The ion solvation state of dimetallic salts of DHA and its derivatives was also studied by UV–VIS spectroscopy. For the dimetallic salts of DHA and its derivatives, their UV–VIS spectra yield two maxima: 305–340 nm and 500–630 nm. However, these absorption bands cannot necessarily be attributed to different ionic triplet moieties. The ratio of peak heights is independent of temperature and is similar for all dimetallic salts of DHA and its derivatives. The latter absorption band changes wavelength with cation radius according to eqn. (2) (Table 1).

$$\lambda_{max} = a + b/r_+ \qquad (2)$$

For dimetallic salts of every dibasic carbon acid studied, except for $DPDHA^{2-}2M^+$, the correlation with cation radius (r_+) is very good. If $DPDHA^{2-}2Li^+$ is excluded this correlation [eqn. (2)] is also good for $DPDHA^{2-}2M^+$. From these results, it may be concluded that the dimetallic salts of DHA and its derivatives exist as CIT in THF at 298 K.[18–21]

The divergence of the $DPDHA^{2-}2Li^+$ absorption from its expected position suggests that it exists as a mixture of CIT and SSIT or MIT. However, another possible explanation is that $DPDHA^{2-}2Li^+$ is a CIT, however, the interionic difference is larger than expected from the lithium cation size. This alternative explanation can be tested by inspecting the temperature dependence of the absorption frequency.

The ion solvation state of the dilithium salts of DHA and its derivatives differs considerably from that of the monolithium salts. For example, monolithium salts of DMDHA and PDHA

Table 1 UV–VIS spectra and correlation parameters ($\lambda_{max} = a + b/r_+$) for dialkali metal salts of DHA and its derivatives in THF

	λ_{max}/nm							
Dianion	Li^+	Na^+	K^+	Rb^+	Cs^+	a^a	b	R^b
DHA^{2-}	570	605	621	626	630	663.4	−56.0	0.999
$MDHA^{2-}$	570	605	623	626	—	665.2	−57.1	0.999
$DMDHA^{2-}$	564	603	624	625	—	669.6	−63.0	0.998
$CNDHA^{2-}$	502	537	552	553	—	590.7	−52.7	0.997
$PDHA^{2-}$	536	563	580	583	—	615.0	−47.8	0.998
$DPDHA^{2-}$	524[c]	529	548	553	554	590.0	−57.0	0.988

[a] The a values correspond to the absorption of free dianions.[23] [b] R is the correlation coefficient of eqn. (2). [c] The absorption for $DPDHA^{2-}2Li^+$ was excluded from the correlation.

are solvent separated ion pairs (SSIP) in THF,[3] while the dimetallic salts exist as CIT. Similarly, monolithium salts of DHA and MDHA exist as a mixture of CIP and SSIP[3,22] but the dilithium salts exist as CIT. Only $CNDHA^-Li^+$ and $CNDHA^{2-}2Li^+$ have similar contact ion structures. Anionic charge appears to be chiefly responsible for these observed differences. It is known that dianion–cation pairs are two orders of magnitude more stable than monoanion–cation pairs.[24] This appears to be the main reason that cation size affects pK_2 more than pK_1.[1]

Temperature effect

Reducing the temperature from 298 K to 225 K does not lead to the appearance of extra peaks in the UV–VIS spectrum but does cause a red shift of both the signals at 300 nm and 600 nm. For the dilithium salts, the λ_{max} in the 600 nm region red shifts by approximately 25 nm. In the 300 nm region, this effect is less than 10 nm. For other dialkali metal salts, the red shift is less than for dilithium salts with virtually no effect on dirubidium salts. The absorption frequencies of dilithium salts at low temperature are similar to those of dicaesium and dirubidium salts at room temperature, and quite different from those of free anions of the same compounds (Table 1). Similar effects have been reported for monometallic salts of these compounds.[3,22]

The observed red shift can be interpreted in two ways.[3,21,25] According to the first model,[21,25] ion triplets of dimetallic salts of DHA and its derivatives exist in two ion solvation states: CIT and SSIT. The energy barrier separating these states is low and the potential wells are shallow. Increasing the temperature changes both the shapes and the depth of the potential wells and the width and height of the barrier. Therefore, the structure of the ion triplets changes gradually from SSIT to CIT with increasing temperature. The two ion triplets interchange very easily because of the low potential barrier. Therefore the UV–VIS spectrum only yields one absorption maximum in the 600 nm range that shifts frequency with temperature. This model can also be applied to MIT formation. The UV–VIS spectrum of such a solution should contain three maxima for CIT, MIT and SSIT. Low energy barriers can similarly be used to explain the appearance of a single peak.

The second model takes into consideration the geometry and electronic structure of the dianion of DHA and its derivatives.[2] The anthracene ring of these dianions is planar with the negative charge concentrated on C-9 and C-10 with some dispersion to C-1, C-2, C-3, C-4, C-5, C-6, C-7 and C-8.[2] In dimetallic salts of DHA and its derivatives, the cations are situated above and below the central benzene ring of the anthracene unit.[7,8,11] The negative charge on carbon atoms of outer rings of the dianions hinders the approach of solvent molecules to cations from all sides except the outer side. Consequently, solvent molecules cannot squeeze between cation and dianion. Therefore, cation solvation only increases

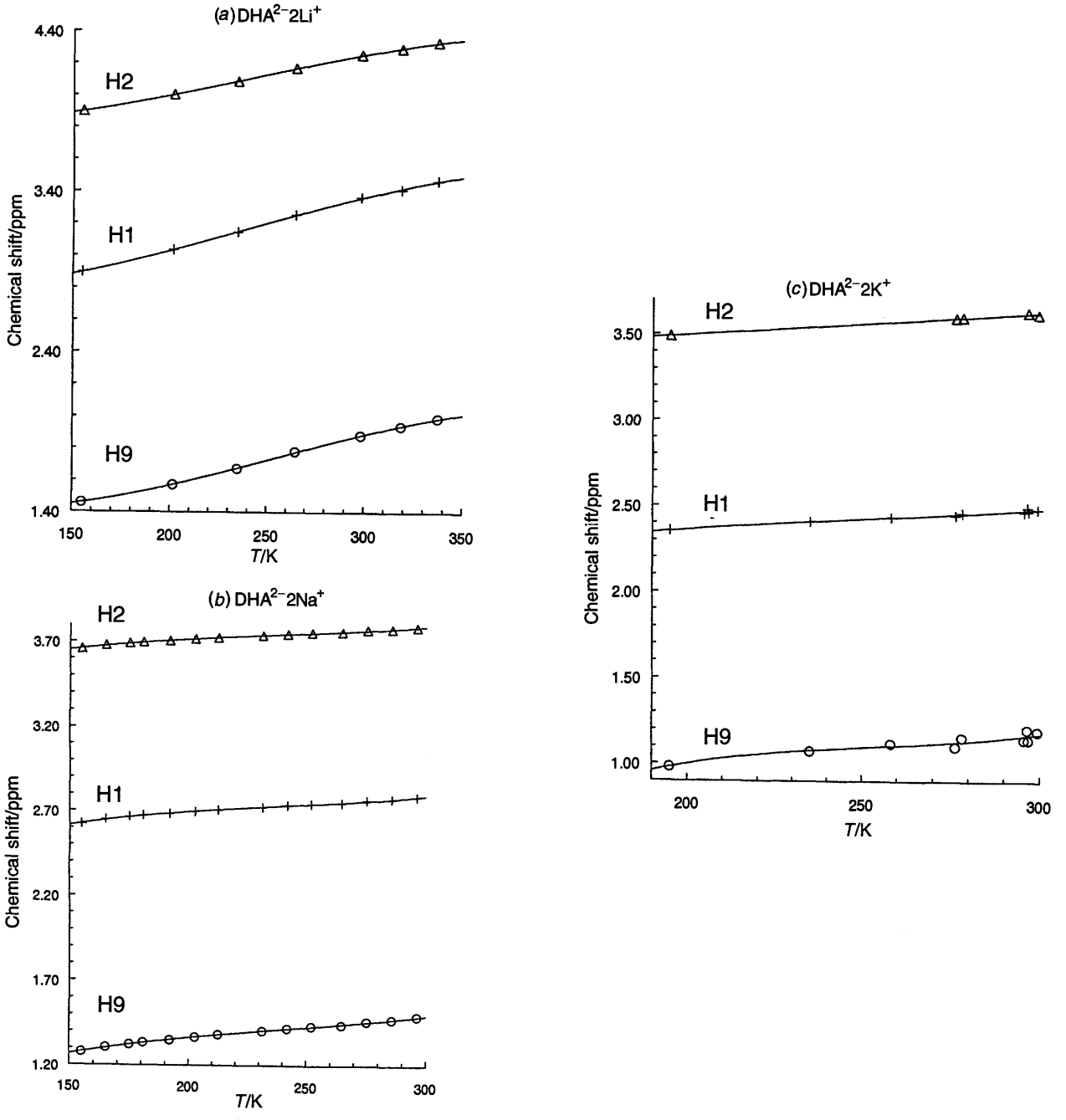

Fig. 2 Temperature dependence of ^{1}H chemical shift of $DHA^{2-}2M^+$; (*a*) M = Li, (*b*) M = Na, (*c*) M = K

interionic distance in CIT but not by enough to form SSIT. This is the reason that the UV–VIS signals of dimetallic salts of DHA and its derivatives red shift as the temperature decreases. According to this view, the $DPDHA^{2-}2Li^+$ is a CIT, with a somewhat increased interionic distance because the lithium cation is surrounded by a large solvent shell but the phenyl substituent moves it away from the dianion plane.

The ^{1}H NMR signals of the dimetallic salts of DHA shift downfield with increasing temperature (Fig. 2). Except for the dilithium salt, the downfield shift is very small. The direction of the change of chemical shift indicates that the interionic distance increases with decreasing temperature. Eqns. (3) and (4) show the correlation of H-1 and H-9 chemical shifts of the dimetallic salts of DHA with cation radius (r_+) at 298 K. These correlations confirm the conclusion that these salts exist as CIT under these conditions.

$$\delta_{H\text{-}1} = 1.799 + 0.938/r_+ \ (R = 0.998) \quad (3)$$

$$\delta_{H\text{-}9} = 0.745 + 0.681/r_+ \ (R = 0.987) \quad (4)$$

The temperature dependence of the carbons of $DHA^{2-}2Na^+$ is very small (Fig. 3). The signs of the dependencies are more indicative of cation coordination in CIT. As the temperature increases, the solvent shell of the cation becomes thinner and its interaction with the nearest coordinated carbon atom increases. This increases the carbon atom's electronic shielding yielding an upfield shift. More distant, uncoordinated, carbons shift downfield. In the ^{13}C spectrum of $DHA^{2-}2Na^+$, only the C-9 signal shifts upfield with increasing temperature, while the others shift downfield (Fig. 3). This shows that the cations of dimetallic salts of DHA are coordinated to the deprotonated carbon atoms: C-9 and C-10.

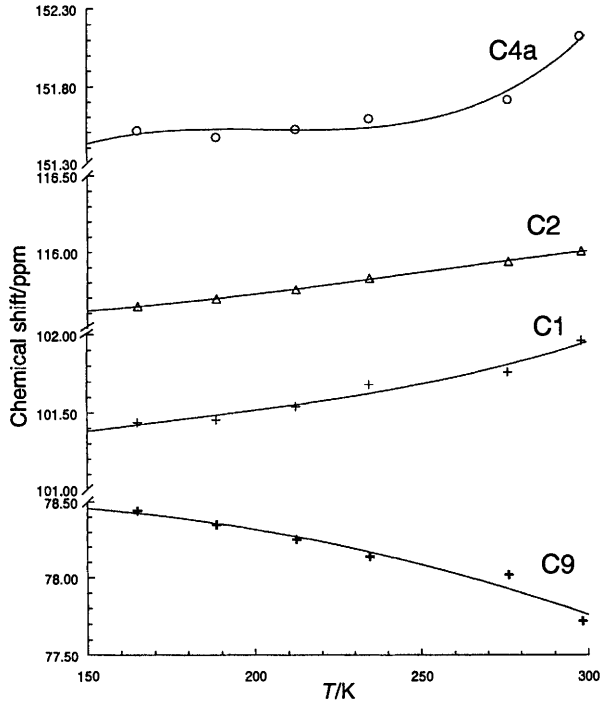

Fig. 3 Temperature dependence of ^{13}C chemical shift of DHA^{2-}-$2Na^+$

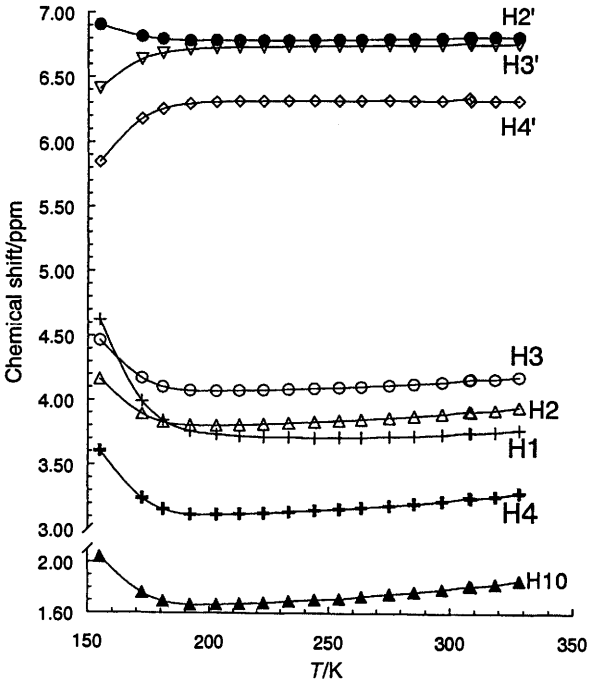

Fig. 4 Temperature dependence of ^1H chemical shift of $PDHA^{2-}$-$2Na^+$

The ^1H and ^{13}C chemical shifts of $MDHA^{2-}2Na^+$, $DMDHA^{2-}2Na^+$ and $CNDHA^{2-}2Na^+$ are practically temperature independent. The H-1 shifts of $MDHA^{2-}2Na^+$, $DMDHA^{2-}2Na^+$ and $CNDHA^{2-}2Na^+$ increase by 0.08 ppm, 0.03 ppm and 0.10 ppm, respectively, as the temperature rises from 165 K to 300 K. It can be deduced from this that the solvation state of these salts does not change over a wide temperature range.

The ^1H and ^{13}C chemical shifts of $PDHA^{2-}2Na^+$ and $DPDHA^{2-}2Na^+$ behave very differently from those of $DHA^{2-}2Na^+$, $MDHA^{2-}2Na^+$, $DMDHA^{2-}2Na^+$ and $CNDHA^{2-}2Na^+$. The chemical shifts of H-1 and H-2 of $PDHA^{2-}2Na^+$ and $DPDHA^{2-}2Na^+$ are very sensitive to temperature change (Figs. 4 and 5). With a temperature increase from 150 K to 180 K, the chemical shift of H-1 decreases from 4.73 ppm to 3.84 ppm and from 6.53 ppm to 4.36 ppm for $PDHA^{2-}2Na^+$ and $DPDHA^{2-}2Na^+$, respectively. The effect on H-2 is smaller being from 4.17 ppm to 3.83 ppm and from 5.67 ppm to 4.34 ppm for $PDHA^{2-}2Na^+$ and $DPDHA^{2-}2Na^+$, respectively. Meanwhile, the phenyl substituents' proton chemical shifts move downfield with increasing temperature (Figs. 4 and 5).

At low temperature (165 K) the chemical shifts of H-1, H-2 and H-4′ for $DPDHA^{2-}2M^+$ correlate well with cation radius (r_+) [eqns. (5)–(7)].

$$\delta_{H\text{-}1}(\text{ppm}) = 2.201 + 2.796/r_+(\text{nm})\ R = 0.983 \quad (5)$$

$$\delta_{H\text{-}2}(\text{ppm}) = 2.558 + 2.537/r_+(\text{nm})\ R = 0.997 \quad (6)$$

$$\delta_{H\text{-}4'}(\text{ppm}) = 6.507 - 0.519/r_+(\text{nm})\ R = 0.995 \quad (7)$$

However, at higher temperatures the correlation does not hold and low correlation coefficients (R) result [eqns. (8) and (9) for $PDHA^{2-}2M^+$ and eqns. (10)–(12) for $DPDHA^{2-}2M^+$

$$\delta_{H\text{-}1}(\text{ppm}) = 2.107 + 1.686/r_+(\text{nm})\ R = 0.803 \quad (8)$$

$$\delta_{H\text{-}2}(\text{ppm}) = 2.440 + 1.534/r_+(\text{nm})\ R = 0.844 \quad (9)$$

$$\delta_{H\text{-}1}(\text{ppm}) = 2.462 + 1.858/r_+(\text{nm})\ R = 0.871 \quad (10)$$

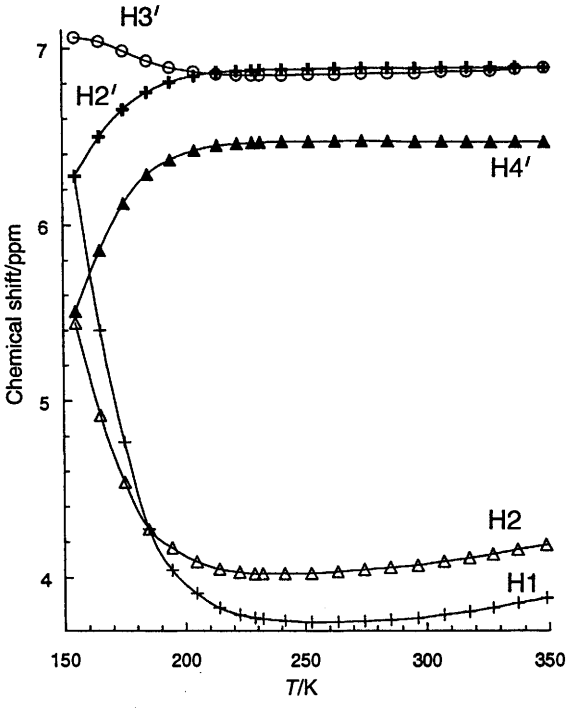

Fig. 5 Temperature dependence of ^1H chemical shift of $DPDHA^{2-}$-$2Na^+$

$$\delta_{H\text{-}2}(\text{ppm}) = 3.303 + 1.210/r_+(\text{nm})\ R = 0.861 \quad (11)$$

$$\delta_{H\text{-}4'}(\text{ppm}) = 6.517 - 0.174/r_+(\text{nm})\ R = 0.538 \quad (12)$$

at 298 K]. We assume that at high temperatures where CIT of $DPDHA^{2-}2M^+$ and $PDHA^{2-}2M^+$ is normally expected, some additional factors of dianion stabilization operate. In order to clarify the nature of these factors we also studied temperature dependence of carbon chemical shifts of $PDHA^{2-}2Na^+$ and $DPDHA^{2-}2Na^+$.

The C-1 resonances of $PDHA^{2-}2Na^+$ and $DPDHA^{2-}2Na^+$ shift strongly upfield with a temperature increase between 165 K and 200 K with little change above that temperature (Figs. 6 and

7). The behaviour of the C-2 resonance is somewhat different. The chemical shift of C-2 of $DPDHA^{2-}2Na^{+}$ is practically independent of temperature while that of $PDHA^{2-}2Na^{+}$ increases slightly with temperature. The C-3 and C-4 resonances of $PDHA^{2-}2Na^{+}$ behave similarly to C-1 although the magnitudes of the shifts are less. The temperature dependence of the C-9 chemical shift is close to that of C-2. The resonances of C-2′ and C-4′ of $DPDHA^{2-}2Na^{+}$ shift downfield with increasing temperature up to 200 K by approximately 7 ppm, while the other substituent carbon chemical shifts show less significant variations with temperature. The chemical shift changes of carbon atoms of the substituent observed for $PDHA^{2-}2Na^{+}$ are smaller than those of $DPDHA^{2-}2Na^{+}$. As for $DPDHA^{2-}2Na^{+}$, the chemical shifts of C-2′ and C-4′ for $PDHA^{2-}2Na^{+}$ also move downfield with increasing temperature but by only approximately 3.5 ppm.

The direction of the NMR resonance shift with temperature for dimetallic salts of phenyl substituted anthracenes differs in principle from that caused by ion-solvation state changes. The NMR resonances of the protons and uncoordinated carbons should shift downfield with increasing temperature. However, the H-1 and H-2 resonances of the lithium and sodium salts shift upfield, although H-3′ and H-4′ resonances shift downfield (Figs. 4 and 5). The chemical shifts of C-1 in $PDHA^{2-}2Na^{+}$ and $DPDHA^{2-}2Na^{+}$ move upfield with increasing temperature although the C-9 resonance of the salts is practically independent of temperature. The C-2′ and C-4′ resonances shift downfield with increasing temperature. The direction of displacement of ^{1}H and ^{13}C chemical shifts of $PDHA^{2-}2Na^{+}$ and $DPDHA^{2-}2Na^{+}$ strongly suggest that they are caused by changes in the p,π-conjugation between the p-electrons of the carbanion centres and the π-electrons of the phenyl substituents. Increased p,π-conjugation, which would occur if the phenyl substituents changed from being tilted out of plane to being in the anthracene plane, would move electron density from the anthracene unit to the phenyl substituents. This would cause a downfield shift of NMR resonances in the anthracene unit and an upfield shift for the phenyl substituents as observed with decreasing temperature.

To check this hypothesis, we carried out semiempirical PM3 calculations. We calculated the dependence of energy and charge distribution in $DPDHA^{2-}$ on the torsion angle between the phenyl substituents' planes and the anthracene unit. The calculations were for symmetrically twisted phenyl substituents. The best conditions for p,π-conjugation occur when the rings are coplanar, *i.e.* the torsion angle is zero. However, there is a global energy minimum at an angle of 42°. We previously determined by AM-1 calculations that the energy of formation was minimum with a torsion angle of 45°.[2]

The electron density at C-1, C-2′, C-4′ and C-9 is more sensitive to the torsion angle than that on C-2, C-8a, C-1′ and C-3′ (Fig. 8). The charge dependencies on C-2′ and C-4′ are similar and in the opposite sense to that on C-1. The charges on C-1′, C-2 and C-8a are much less dependent on torsion angle. The charge on C-9 behaves in a more complex fashion. As the torsion angle increases from 0° to 45°, the charge on C-9 varies little but rises sharply as the torsion angle increases to 90°. The dependence of charge distribution on C-1, C-2, C-2′, C-4′ and C-9 on torsion angle mirrors the temperature dependence of the ^{13}C chemical shifts (*cf.* Figs. 5 and 7). This similarity confirms the hypothesis that the unusual temperature dependencies of chemical shifts for dianions of phenyl substituted anthracenes are caused by a change in orientation of the phenyl substituents.

Increasing temperature alone cannot change the substituent orientation.[26] However, temperature changes influence cation solvation and, therefore, cation–anion distance in dimetallic salts. At high temperatures, the cation is poorly solvated and is situated near the deprotonated carbon atom. This prevents the phenyl substituent from occupying an optimal orientation for

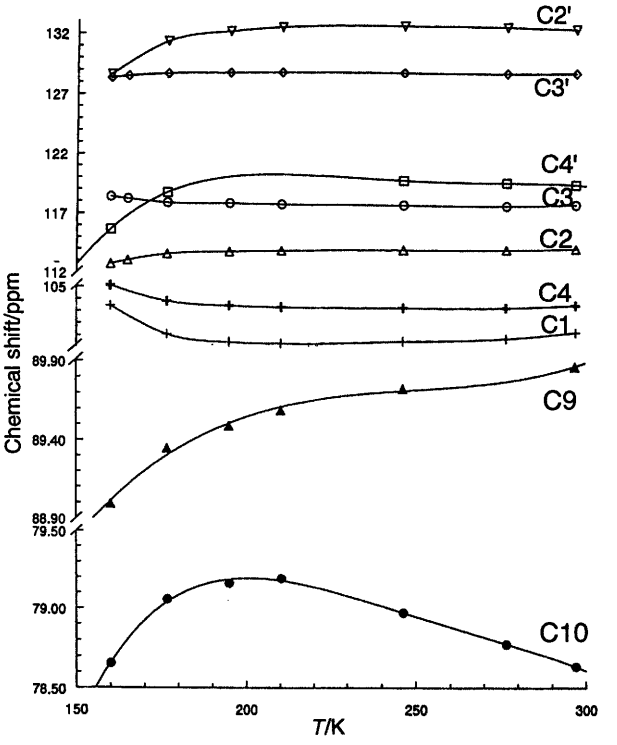

Fig. 6 Temperature dependence of ^{13}C chemical shift of $PDHA^{2-}2Na^{+}$

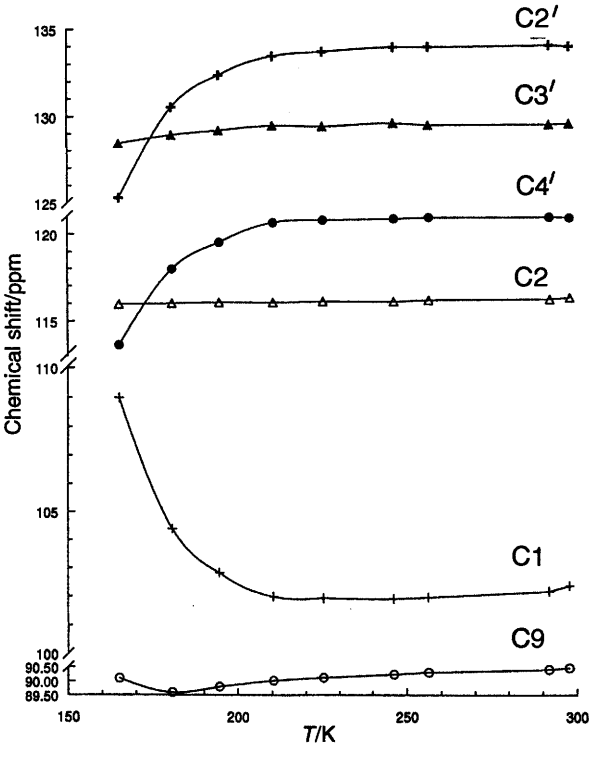

Fig. 7 Temperature dependence of ^{13}C chemical shift of $DPDHA^{2-}2Na^{+}$

p,π-conjugation and therefore the negative charge is concentrated on the anthracene unit. As a result, the C-1 and C-9 resonances are shifted upfield. At low temperatures, the cation is well solvated and further from the carbanion centre allowing the phenyl substituent to occupy a more favourable position for p,π-conjugation. Negative charge is displaced from the anthracene unit towards the phenyl substituents. As a result, the anthracene carbon resonances shift downfield while the phenyl carbon resonances shift upfield.

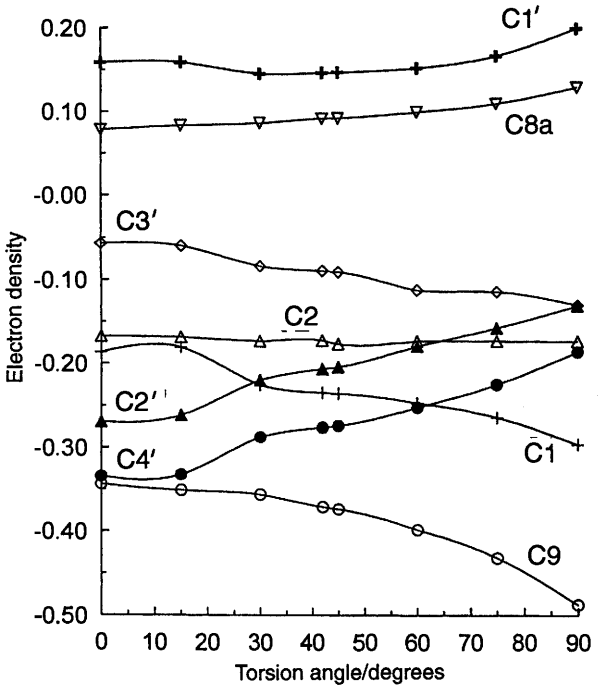

Fig. 8 Dependence of electron density on carbon atoms of $DPDHA^{2-}$ upon torsion angle between the phenyl substituents and anthracene planes

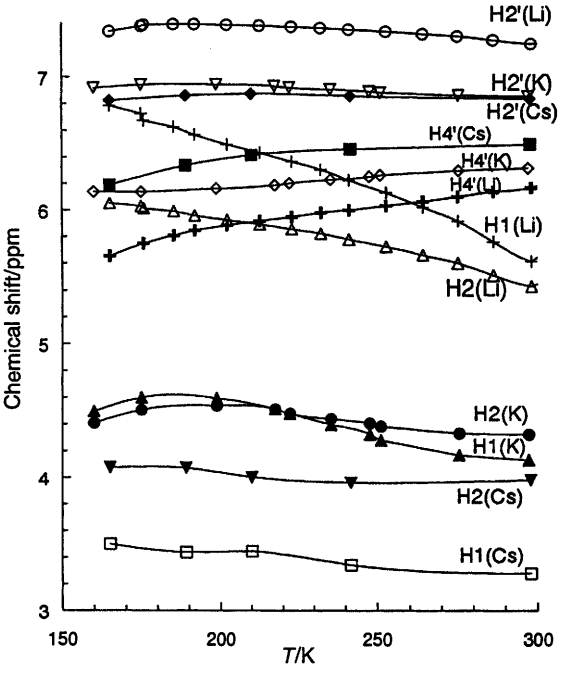

Fig. 9 Temperature dependence of ^1H chemical shift of $DPDHA^{2-}2Li^+$, $DPDHA^{2-}2K^+$ and $DPDHA^{2-}2Cs^+$

THF solvates lithium and sodium cations well. Their solvation shell weakens sharply with increasing temperature. Therefore, the above phenomena are clear for the lithium and sodium salts. The effect is less pronounced for potassium and caesium salts as their cations are poorly solvated and the effect on their chemical shifts much less (Figs. 5 and 9).

Structure of $PDHA^{2-}2Li^+$ and $DPDHA^{2-}2Li^+$ (PM3 calculation)

We examined six possible structures for $PDHA^{2-}2Li^+$ and $DPDHA^{2-}2Li^+$ (Table 2). The structures differ with respect to the location of the cation. The energy of formation (ΔH_f), charge distribution and geometry of the structures were calculated by the PM3 method[13] with Thiel's lithium parameters.[27] We fixed the cation location relative to the anion but all other internal degrees of freedom were optimized. All the structures considered are in the ground state. Previously, Rabideau *et al.*[11] reported the results of MNDO calculations for $DHA^{2-}2Li^+$ that are included in Table 2 for comparison. The order of stability is as follows, the structure number being taken from Table 2.

$$DHA^{2-}2Li^+: \mathbf{1} < \mathbf{2} < \mathbf{3} < \mathbf{4} < \mathbf{5} < \mathbf{6}$$

$$PDHA^{2-}2Li^+: \mathbf{1} < \mathbf{2} < \mathbf{3} < \mathbf{5} < \mathbf{4} < \mathbf{6}$$

$$DPDHA^{2-}2Li^+: \mathbf{5} < \mathbf{1} < \mathbf{6} < \mathbf{4} < \mathbf{2} < \mathbf{3}$$

Structures with lithiums either side of the anion plane are more stable than those with lithiums on the same side (Table 2). The orders of stability for $DHA^{2-}2Li^+$ and $PDHA^{2-}2Li^+$ are similar with one major exception. For $PDHA^{2-}2Li^+$, structure **5** with the cations on the outer rings, is more stable than structure **4** with one cation on the central ring. This is the opposite of $DHA^{2-}2Li^+$. The most stable structure of $DHA^{2-}2Li^+$ and $PDHA^{2-}2Li^+$ is structure **1** that has one cation on the central ring and one on an outer ring on the opposite side of the anion plane. This corresponds to the X-ray crystal structure of dilithium 9,10-dihydroanthracenediide bis-(tetramethylenediamine).[10] According to Rabideau's calculations,[11] such a structure is the most stable for all dilithium salts of polynuclear aromatics. However, we find that the most stable structure for $DPDHA^{2-}2Li^+$ was structure **5** with both lithiums on opposite sides on the outer rings. Notwithstanding, structures **5** and **6** for $DHA^{2-}2Li^+$ and $PDHA^{2-}2Li^+$ are the least stable. This difference is undoubtedly due to the presence of the phenyl substituents.

Cation–anion interaction and/or p,π-conjugation of the carbanion centres' p-electrons with the phenyl substituents' π-electrons can stabilize the negative charge of dianions. For p,π-conjugation the phenyl groups must be coplanar with the anthracene unit. Location of the cation on the central ring hinders such coplanarity. Additionally, the covalency of the lithium–carbon bond is rather high[28] so the deprotonated carbon atoms for structures **1**, **3** and **4** have some sp^3 character.

Tables 3 and 4 show the net charge on the carbons and cations of $PDHA^{2-}2Li^+$ and $DPDHA^{2-}2Li^+$ along with the angles α and γ, which are closest to the optimum (both zero) for p,π-conjugation for structures **2** and **5**. In structures **2** and **5**, both cations are situated on the benzene rings of the anthracene unit so they hinder coplanarity less than for structures **1**, **3** and **4**. The negative charge on the substituents would also be expected to be larger for structures **2**, **5** and **6** than for structures **1**, **3** and **4**. The calculated charges for the $DPDHA^{2-}2Li^+$ phenyl substituents are 1.051, 1.040 and 1.021 for structures **2**, **5** and **6** while for structures **1**, **3** and **4** the charges are 0.972, 0.954 and 1.008, respectively. The same relationship is observed for $PDHA^{2-}2Li^+$.

Our calculations of structure of the dilithium salts apply to the gas phase and therefore overrate the stabilization of the salts caused by covalency of the carbon–lithium bond. Nevertheless, our results show that p,π-conjugation reduces the energy more than direct interaction of the cations with the carbanion centres. In THF solution where solvent molecules surround the cation, its interaction with the dianon is less than that in the gas phase. Therefore, in solution, the dianion stabilization by p,π-conjugation must be larger than that by the cation–dianion interaction.

Conclusions

Dimetallic salts of DHA and its derivatives exist as contact ion triplets (CIT) in THF solution. CIT of these salts do not transform into solvent separated ion triplets (SSIT) with

Table 2 Position of lithium cations with respect to the benzene rings of the anthracene unit and their energies of formation (ΔH_f)

Structure number	Structure	Energy of formation ΔH_f/kcal mol^{-1} [a]		
		$DHA^{2-}2Li^+$	$PDHA^{2-}2Li^+$	$DPDHA^{2-}2Li^+$
1		12.3	136.2	167.6
2		15.9	137.3	173.5
3		16.2	137.7	179.5
4		18.7	139.3	170.7
5		19.5	138.4	167.3
6		21.5	139.9	168.9

[a] 1 cal = 4.184 J.

decreasing temperature (to 165 K). However, the distance between the cations and the dianion increases with decreasing temperature. The mechanism of dianion charge stabilization for $PDHA^{2-}2M^+$ and $DPDHA^{2-}2M^+$ differs from that of $DHA^{2-}2M^+$, $MDHA^{2-}2M^+$, $DMDHA^{2-}2M^+$ and $CNDHA^{2-}2M^+$. Cation–dianion interaction stabilizes the negative charge of the latter group.

Both p,π-conjugation of the charge at the carbanion centres with the phenyl substituents and cation–dianion interaction stabilize $PDHA^{2-}2M^+$ and $DPDHA^{2-}2M^+$. Both stabilization factors compete. The contribution of p,π-conjugation to the stabilization increases with decreasing temperature.

Experimental

^1H and ^{13}C NMR spectra were recorded on a Bruker AMX-400 spectrometer in [$^2H_8$]THF. As alkali metal anions react with tetramethylsilane (TMS), the chemical shifts were referenced to the most downfield solvent peaks, which are the better resolved signals of the solvent. The chemical shifts were determined from the multiplets' centres of gravity. The solvent chemical shifts were determined for pure [$^2H_8$]THF (99.65% atom D) containing TMS (< 5 mmol dm^{-3}). Varying the concentration of TMS up to 5 mmol dm^{-3} had no perceptible (< 0.001 ppm) effect on the chemical shift. The temperature was determined using a standard methanol NMR thermometer at temperatures up to 340 K and a standard ethylene glycol thermometer for higher temperatures.[29,30] In the temperature range 155–390 K, the chemical shift of the 1-H of [$^2H_7$]THF in [$^2H_8$]THF was found to be $3.5749 + (4.71 \times 10^{-5}\ T') - (5.1 \times 10^{-8}\ T'^2) + (8.2 \times 10^{-10}\ T'^3) - (3.3 \times 10^{-12}\ T'^4)$ ppm. The chemical shift of C-1 of [$^2H_8$]THF (155–340 K) was found to be $67.3937 + (8.242 \times 10^{-4}\ T') + (6.6281 \times 10^{-6}\ T'^2) + (1.65 \times 10^{-9}\ T'^3)$ ppm where T' is temperature, 295 K. The standard deviations of error for the chemical shifts were 0.0003 and 0.0009 ppm for ^1H and ^{13}C, respectively.[2]

Assignments of the ^{13}C spectra were made using ^1H detected ^1H–^{13}C correlation spectroscopy.[31] The ^1H NMR spectrum was assigned, either by simple inspection or by NOESY.[32] Assignment of quaternary carbons was often straightforward, but where there was uncertainty, long-range ^1H detected ^1H–^{13}C correlation spectroscopy[33] was used.

Materials

Commercial samples of anthracene, 9,10-dihydroanthracene, 9-methylanthracene, 9,10-dimethylanthracene, 9-phenylanthracene, 9,10-diphenylanthracene and 9-cyanoanthracene were purified by multiple recrystallization (methanol) and/or vacuum sublimation. Alkali metals were of commercial origin.

[$^2H_8$]THF. The commercial solvent was prepared as previously reported.[3] The [$^2H_8$]THF was placed in a flask equipped with a vacuum line, then degassed in several freeze-pump thaw cycles before being vacuum transferred into a flask containing distilled Na:K, 5:1, alloy. This was then sonicated until a blue colour developed. The flask was allowed to stand overnight then sonicated again until a permanent blue colour developed. The solvent was then vacuum transferred to another flask containing distilled Na–K alloy.

Data concerning anthracene, 9,10-dihydroanthracene (DHA), 9-methylanthracene, 9-cyanoanthracene, 9-phenylanthracene, 9,10-dimethylanthracene, 9,10-diphenylanthracene and disodium salts of 9,10-dihydroanthracene (DHA), 9-methyl-9,10-dihydroanthracene (MDHA), 9-cyano-9,10-dihydroanthracene (CNDHA), 9-phenyl-9,10-dihydroanthracene (PDHA), 9,10-dimethyl-9,10-dihydroanthracene (DMDHA), 9,10-diphenyl-9,10-dihydroanthracene (DPDHA) appear in ref. 2.

Dilithium 9,10-dihydroanthracenediide. δ_H([$^2H_8$]THF, 298 K, 10–13 mmol dm^{-3}) 1.41 (s, 2 H, 9-H) and 2.81 (1-H) and 3.84 (2-H) (AA'XX', each 4 H).

Dipotassium 9,10-dihydroanthracenediide. δ_H([$^2H_8$]THF, 195.0–299.4 K, 0.15–0.17 mmol dm^{-3}) 1.17 (s, 2 H, 9-H) and 2.48 (1-H) and 3.62 (2-H) (AA'XX', each 4 H).

Dirubidium 9,10-dihydroanthracenediide. δ_H([$^2H_8$]THF, 297.2 K, 0.05 mmol dm^{-3}) 1.18 (s, 2 H, 9-H) and 2.41 (1-H) and 3.59 (2-H) (AA'XX', each 4 H).

Dicaesium 9,10-dihydroanthracenediide. δ_H([$^2H_8$]THF, 297.2 K, 0.05 mmol dm^{-3}) 1.21 (s, 2 H, 9-H) and 2.39 (1-H) and 3.70 (2-H) (AA'XX', each 4 H).

Dilithium 9-phenyl-9,10-dihydroanthracenediide. δ_H([$^2H_8$]-THF, 296.8 K) 2.58 (s, 1 H, 10-H), 4.40 (d, 2 H, 4-H), 5.07 (t, 2 H, 3-H), 4.89 (d, 2 H, 1-H), 5.27 (t, 2 H, 2-H), 6.11 (t, 1 H, 4'-H), 6.63 (d, 2 H, 3'-H) and 7.10 (t, 1 H, 2'-H).

Dipotassium 9-phenyl-9,10-dihydroanthracenediide. δ_H([$^2H_8$]-THF, 298 K) 1.81 (s, 1 H, 10-H), 3.18 (d, 2 H, 4-H), 4.29 (d, 2 H, 1-H), 4.19 (t, 2 H, 2-H), 4.16 (t, 2 H, 3-H), 5.90 (t, 1 H, 4'-H), 6.68 (t, 2 H, 3'-H) and 6.83 (d, 2 H, 2'-H).

Dirubidium 9-phenyl-9,10-dihydroanthracenediide. δ_H([$^2H_8$]-THF, 298 K) 1.80 (d, 2 H, 4-H), 3.77 (d, 2 H, 1-H), 3.93 (t, 2 H, 2-H), 4.18 (t, 2 H, 3-H), 6.20 (t, 1 H, 4'-H), 6.67 (t, 2 H, 3'-H) and 6.79 (d, 2 H, 2'-H).

Dicaesium 9-phenyl-9,10-dihydroanthracenediide. δ_H([$^2H_8$]-THF, 298 K) 1.45 (s, 1 H, 10-H), 2.75 (d, 2 H, 4-H), 2.84 (d, 2 H, 1-H), 3.73 (t, 2 H, 3-H), 6.45 (t, 1 H, 4'-H), 6.89 (t, 2 H, 3'-H), 6.71 (d, 2 H, 2'-H).

Table 3 Net charge on carbon atoms and cations for different structures of dilithium 9-phenyl-9,10-dihydroanthracene as well as angles between the planes of anthracene and the phenyl

Structure	Charge														α	γ
	C-1	C-2	C-3	C-4	C-4a	C-8a	C-9	C-10	C-1′	C-2′	C-3′	C-4′	Li-1	Li-2		
	−0.301	−0.113	−0.130	−0.290	0.130	0.027	−0.344	−0.379	0.063	−0.115	−0.103	−0.124	0.452	0.390	89.44	8.89
	−0.357	−0.132	−0.130	−0.361	0.099	0.038	−0.216	−0.257	0.038	−0.107	−0.108	−0.122	0.416	0.387	76.50	1.40
	−0.167	−0.092	−0.167	−0.113	0.082	0.082	−0.360	−0.384	0.065	−0.116	−0.104	−0.126	0.422	0.396	73.46	2.70
	−0.266	−0.101	−0.148	−0.227	0.130	0.027	−0.306	−0.358	0.048	−0.109	−0.109	−0.122	0.419	0.253	68.19	6.74
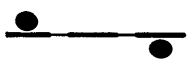	−0.217	−0.179	−0.081	−0.286	0.098	0.129	−0.343	−0.399	0.063	−0.120	−0.107	−0.130	0.429	0.430	69.78	0.53
	−0.212	−0.175	−0.078	−0.282	0.096	0.127	−0.333	−0.388	0.062	−0.125	−0.109	−0.128	0.403	0.403	73.06	3.45

Table 4 Net charge on carbon atoms and cations for different structures of dilithium 9,10-diphenyl-9,10-dihydroanthracene as well as angles between the planes of anthracene and the phenyl

Structure	Charge										
	C-1	C-2	C-4a	C-9	C-1′	C-2′	C-3′	C-4′	Li^+	α	γ
	−0.293	−0.121	0.129	−0.352	0.067	−0.117	−0.102	−0.124	0.432	70.2	9.9
	−0.301	−0.330	0.050	−0.124	0.018	−0.101	−0.110	−0.118	0.378	82.0	3.0
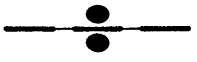	−0.183	−0.129	0.048	−0.385	0.069	−0.106	−0.103	−0.121	0.477	81.9	11.8
	−0.249	−0.124	0.124	−0.323	0.052	−0.113	−0.102	−0.122	0.350	68.6	6.7
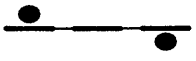	−0.254	−0.128	0.119	−0.356	0.064	−0.120	−0.107	−0.129	0.437	71.8	0
	−0.233	−0.147	0.108	−0.344	0.062	−0.107	−0.105	−0.127	0.412	73.9	4.0

Dipotassium 9,10-dimethyl-9,10-dihydroanthracenediide. δ_H([$^2H_8$]THF, 298 K) −0.11 (s, 6 H, 1′-H) and 2.88 (1-H) and 4.02 (2-H) (AA′XX′, each 4 H).

Dilithium 9,10-diphenyl-9,10-dihydroanthracenediide. δ_H([$^2H_8$]THF, 298 K, 0.54–409 mmol dm^{-3}) 5.51 (2-H) and 5.80 (1-H) (AA′XX′, each 4 H), 6.19 (t, 2 H, 4′-H), 6.75 (t, 4 H, 3′-H) and 7.28 (2′-H); δ_C([$^2H_8$]THF, 297 K, 1.4–409 mmol dm^{-3}) 84.0 (C-9), 113.9 (C-1), 115.0 (C-4′), 116.4 (C-2), 124.0 (C-2′), 128.8 (C-3′), 145.7 (C-4a) and 145.0 (C-1′).

Dipotassium 9,10-diphenyl-9,10-dihydroanthracenediide. δ_H([$^2H_8$]THF, 297 K, 0.06–2.9 mmol dm^{-3}) 4.13 (1-H) and 4.32 (2-H) (AA′XX′, each 4 H), 6.13 (t, 2 H, 4′-H), 6.64 (t, 4 H, 3′-H) and 6.85 (d, 4 H, 2′-H); δ_C([$^2H_8$]THF, 298.1 K) 102.2 (C-9), 105.7 (C-1), 117.0 (C-2), 119.0 (C-4′), 129.8 (C-3′), 130.9 (C-2′), 146.5 (C-1′) and 147.8 (C-4a).

Dirubidium 9,10-diphenyl-9,10-dihydroanthracenediide. δ_H([$^2H_8$]THF, 298 K, 0.18–2.6 mmol dm^{-3}) 4.3 (1-H) and 4.06 (2-H) (AA′XX′, each 4 H), 6.18 (t, 2 H, 4′-H), 6.78 (t, 4 H, 3′-H) and 6.88 (d, 4 H, 2′-H).

Dicaesium 9,10-diphenyl-9,10-dihydroanthracenediide. δ_H([$^2H_8$]THF, 298 K, 0.1 mmol dm^{-3}) 3.28 (1-H) and 4.07 (2-H) (AA′XX′, each 4 H), 5.86 (t, 2 H, 4′-H), 6.18 (t, 4 H, 3′-H) and 6.84 (d, 4 H, 2′-H).

Acknowledgements

We thank the US–Israel binational science foundation for financial support and the Margaret Thatcher Center of Interdepartmental Scientific Equipment for NMR facilities.

References

1 I. O. Shapiro, M. Nir, R. E. Hoffman and M. Rabinovitz, *J. Chem. Soc., Perkin Trans. 2*, 1994, 1519.
2 M. Nir, R. E. Hoffman, I. O. Shapiro and M. Rabinovitz, *J. Chem. Soc., Perkin Trans. 2*, 1995, 1433.
3 R. E. Hoffman, M. Nir, I. O. Shapiro and M. Rabinovitz, *J. Chem. Soc., Perkin Trans. 2*, 1996, 1225.
4 R. B. Bates, *Comprehensive Carbanion Chemistry*, eds. E. Buncel and T. Durst, Elsevier, Amsterdam, part A, ch. 1, 1980.
5 C. M. Thompson and D. L. C. Green, *Tetrahedron*, 1991, **47**, 4223.
6 E. S. Petrov, M. I. Terekhova and A. I. Shatenstein, *Russ. Chem. Rev.*, 1973, **42**, 1574.
7 A. Streitwieser, *Acc. Chem. Res.*, 1984, **17**, 353.
8 A. Streitwieser, C. M. Berke and K. Robbers, *J. Am. Chem. Soc.*, 1978, **100**, 8271.
9 A. Streitwieser, E. Juarists and L. L. Nebenzahl, *Comprehensive Carbanion Chemistry*, eds. E. Buncel and T. Durst, Elsevier, Amsterdam, part A, ch. 7, 1980.
10 W. E. Rhine, J. J. Brooks and G. D. Stucky, *J. Am. Chem. Soc.*, 1975, **97**, 2079.
11 A. Sygula, K. Lipkowitz and P. W. Rabideau, *J. Am. Chem. Soc.*, 1987, **109**, 6602.
12 P. W. Rabideau, *Tetrahedron*, 1989, **45**, 1579.
13 J. J. P. Stewart, *J. Comp. Chem.*, 1989, **10**, 210.
14 R. H. Cox, L. W. Harrison and W. K. Austin, *J. Chem. Phys.*, 1977, **77**, 200.
15 G. L. Collins, T. E. Hogen-Esch and J. Smid, *J. Solution. Chem.*, 1978, **7**, 9.
16 U. Takaki, G. L. Collins and J. Smid, *J. Organomet. Chem.*, 1978, **145**, 139.
17 D. H. O'Brien, C. R. Russell and A. J. Hart, *J. Am. Chem. Soc.*, 1976, **98**, 7427.
18 T. E. Hogen-Esch and J. Smid, *J. Am. Chem. Soc.*, 1966, **88**, 307.
19 J. Smid, *Ions and Ion Pairs in Organic Reactions*, ed. M. Szwarc, Wiley, New York, **1**, ch. 3 (1972).
20 T. E. Hogen-Esch, *Adv. in Phys. Org. Chem.*, 1977, **15**, 153.
21 M. Szwarc, *Ions and Ion Pairs in Organic Reactions*, ed. M. Szwarc, Wiley, New York, 1972, vol. 1, ch. 1.
22 D. Nicholls and M. Szwarc, *Proc. Roy. Soc. A*, 1967, **301**, 223.
23 L. Xie and A. Streitweiser, *J. Org. Chem.*, 1995, **60**, 1339.
24 A. J. Fry, *Synthetic Organic Electrochemistry*, Harper and Row, New York, 1972, pp. 136–9; 258–61.
25 P. Chang, R. V. Seates and M. Szwarc, *J. Phys. Chem.*, 1966, **70**, 3180.
26 W. Huber and K. Müllen, *Acc. Chem. Res.*, 1986, **19**, 300.
27 W. Thiel, *QCPE Catalog*, 1983, **15**, 438.
28 H. F. Ebel, *Tetrahedron*, 1968, **24**, 459.
29 A. L. Van Geet, *Anal. Chem.*, 1968, **40**, 2227.
30 A. L. Van Geet, *Anal. Chem.*, 1970, **42**, 679.
31 A. Bax and S. Subramanian, *J. Magn. Reson.*, 1986, **67**, 565.
32 G. Bodenhausen, H. Kogler and R. R. Ernst, *J. Magn. Reson.*, 1986, **58**, 370.
33 A. Bax and M. F. Summer, *J. Am. Chem. Soc.*, 1986, **108**, 2093.

Paper 6/01070I
Received 13*th February* 1996
Accepted 1*st April* 1996